ELSEVIER

Journal of Alloys and Compounds 293–295 (1999) 88–92

Journal of ALLOYS AND COMPOUNDS

Structural studies of Laves phases $ZrCo(V_{1-x}Cr_x)$ with $0 \leq x \leq 1$ and their hydrides

J.L. Soubeyroux*, D. Fruchart, A.S. Biris[1]

Laboratoire de Cristallographie du CNRS, associé à l'Université J. Fourier, BP 166, 38042 Grenoble Cedex 09, France

Abstract

Laves phases of the series $ZrCo(V_{1-x}Cr_x)$ with $0 \leq x \leq 1$ have been synthesised with the hexagonal C14-type structure. We have analyzed the structure of the alloys by X-ray and neutron diffraction, and determined the sites occupied by transition metals with the V/Cr substitution. The positions of hydrogen atoms in the structure and the occupation of the different interstitial sites of the hydrides have been determined. The effects of the V/Cr substitution have been studied with regard to the phase stability, the maximum hydrogen content and the hydrogen site stability. *P–c–T* measurements show a good reversibility of the hydrogen uptake.

Keywords: Laves phases; $ZrCo(V_{1-x}Cr_x)$; Hydrides; Neutron diffraction; Metal hydrogen systems

1. Introduction

Alloys based on the Laves phase system $Zr(M_{1-x}M'_x)_2$ where M and M′ are 3d transition metals were investigated as potential hydrogen storage materials [1–15]. These intermetallic compounds exhibit interesting properties for hydrogen storage: large hydrogen capacities ($ZrV_2H_{5.2}$, $ZrCr_2H_{3.4}$ [2], $ZrMn_2H_{3.6}$ [3]), easy activation, fast kinetics.

The aim of our systematic studies is to determine the position and the distribution of the substituted metal elements in the structure as driving parameters on the hydrogen storage characteristics. Then after the measurement of the maximum hydrogen absorption capacity, we study the hydriding–dehydriding properties by analysis of the pressure–composition–temperature behaviour. On the basis of all these characteristics, hydrogen location and occupation of the possible interstitial sites are determined and discussed [16–22].

In this paper, we present the results obtained from X-ray and neutron diffraction for alloys and hydrides for the series $ZrCoV_{1-x}Cr_x$ with $0 \leq x \leq 1$ and *P–c–T* measurements for the composition $ZrCoV_{0.2}Cr_{0.8}$. We discuss the influence of the chromium content on the B metal sites (2a and 6h) and its impact on the size of the interstitial sites available for hydrogen.

2. Experimental details

The starting elements (3*N* purity) were melted by using the HF induction furnace technique, in a cold copper crucible under argon atmosphere (5*N*). The alloys were crushed in a stainless steel mortar and sieved under 200 μm. In order to prepare the hydrides with the maximum hydrogen content, the powders were placed into silica tubes and then into a stainless steel autoclave able to work under several ten atmospheres of hydrogen gas pressure and up to 800°C. After several evacuation and H_2 rinsing cycles, hydrogen gas was admitted into the reactor at 1 MPa pressure. In order to activate the absorption process, a first hydriding cycle was performed by slowly increasing temperature until hydrogen absorption occurs. After this first hydrogen uptake, the reactor was evacuated and the sample was cooled down to room temperature. The procedure was repeated and when hydrogen absorption started, temperature was kept constant and the H_2 gas pressure increased to 2 MPa in order to reach the maximum hydrogen charge. Then the sample was cooled down to room temperature under hydrogen pressure. The amount

*Corresponding author.

[1]Present address: Institut of Isotopic and Molecular Technology, P.O. Box 700, R-3400 Cluj-Napoca, Romania.

0925-8388/99/$ – see front matter
PII: S0925-8388(99)00305-9

of the hydrogen uptake was measured by weighing the alloy before the experiment and the hydride after the reaction.

All the samples (alloys and hydrides) were analysed by powder X-ray diffraction using a Philips diffractometer (λ_{Cu}=1.5406 Å) equipped with a backscattering graphite monochromator. The neutron diffraction experiments were carried out at the RHF reactor of ILL on the D1B powder diffractometer which is equipped with a 400 cells position sensitive detector, covering a 80°–2Θ range. The wavelength used was 1.288 Å from a germanium monochromator. The diffraction patterns were analysed by using the FULLPROF profile refinement software [23]. Deuterium rather than hydrogen has been used to study the hydrides in order to reduce the incoherent absorption and diffusion of neutrons.

The pressure–composition isotherms (P–C–T) were measured using a thermogravimetric system described previously [24].

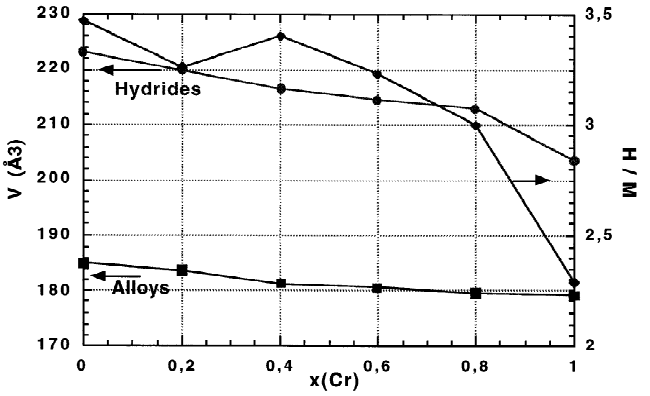

Fig. 1. Unit cell volume variation of the $ZrCoV_{1-x}Cr_x$ with $0 \leq x \leq 1$ as-cast alloys and hydrides versus chromium content. (Plain squares and circles for volumes, open squares for H/M content).

3. Results and discussion

3.1. Structural parameters of the $ZrCo(V_{1-x}Cr_x)$ alloys

All the as cast alloys prepared in the composition range $0 \leq x \leq 1$ crystallise in the hexagonal C14-type structure. Table 1 reports the cell parameters determined by X-ray and neutron diffraction and the maximum hydrogen capacities measured from the weighing procedure.

The cell volume variation of the C14 alloys is in good agreement with the metal radius variation. Effectively a vanadium atom (r=1.34 Å) is replaced by a smaller chromium one (r=1.30 Å). The decrease of the unit cell volume versus the chromium content is reported in Fig. 1.

Structural refinements of powder neutron diffraction patterns recorded on the C14 as cast alloys have confirmed the structure of these phases. The refinement processes were performed in the $P6_3/mmc$ space group, the results are reported in Table 2. For example, Fig. 2a shows the experimental and calculated diffraction patterns for the $ZrCoV_{0.2}Cr_{0.8}$ compound. In these refinements, as there are three elements to locate on two sites, the cobalt and the chromium having positive and close scattering lengths, the vanadium having a low and negative scattering length, we have fixed a statistical occupation for the cobalt and refined the two others. As reported in Fig. 3(a,b), we found that there is a fully statistical occupation of the three elements on both sites 2a and 6h. This procedure can be subject to criticism as one parameter is fixed in the refinement, but in the compounds with only two elements on the two sites (ZrCoV and ZrCoCr) we have not evidenced any preferred site occupation in the powder neutron refinements.

3.2. Structural parameters of the $ZrCo(V_{1-x}Cr_x)H_y$ hydrides (deuterides)

From the X-ray and neutron diffraction patterns it is shown that the hydrides retain the structure of the hexagonal C14 parent alloys. The hydrogen absorption capacity determined from the weighing procedure is nearly constant up to a chromium content of 0.8, then it decreases. The volume increase from the different alloys to the corresponding hydrides is ranging from 18.5 to 20.6% for the hydrides having an hydrogen capacity above 3 H/f.u. but only up to 13.7% for the hydride having the lower capacity (2.3 H/f.u.).

The structural refinements of the neutron diffraction patterns of the hydrides have been done using the same

Table 1
Cell parameters and hydrogen maximum capacity of alloys and hydrides synthesised with the C14-type structure ($\Delta a = 2.10^{-3}$ Å and $\Delta c = 3.10^{-3}$ Å)

	Alloys			Hydrides				
	a (Å)	c (Å)	V (Å^3)	N_H	a (Å)	c (Å)	V (Å^3)	$\Delta V/V$ (%)
ZrCoV	5.077	8.289	185.03	3.46	5.404	8.821	223.08	20.57
$ZrCo(V_{0.8}Cr_{0.2})$	5.065	8.275	183.84	3.26	5.376	8.788	219.95	19.64
$ZrCo(V_{0.6}Cr_{0.4})$	5.0405	8.241	181.32	3.40	5.347	8.745	216.52	19.41
$ZrCo(V_{0.4}Cr_{0.6})$	5.032	8.2356	180.59	3.23	5.330	8.719	214.51	18.78
$ZrCo(V_{0.2}Cr_{0.8})$	5.0201	8.2254	179.51	3.00	5.316	8.694	212.77	18.53
ZrCoCr	5.0109	8.2341	179.05	2.29	5.237	8.571	203.62	13.72

Table 2
Neutron diffraction structure refined parameters of the as-cast hexagonal C14 alloys and their hydrides for $0 \leq x \leq 0.8$

Compound	ZrCoV	$ZrCoVD_x$	$ZrCoV_{0.8}Cr_{0.2}$	$ZrCoV_{0.8}Cr_{0.2}D_x$	$ZrCoV_{0.6}Cr_{0.4}$	$ZrCoV_{0.6}Cr_{0.4}D_x$	$ZrCoV_{0.4}Cr_{0.6}$	$ZrCoV_{0.4}Cr_{0.6}D_x$	$ZrCoV_{0.2}Cr_{0.8}$	$ZrCoV_{0.2}Cr_{0.8}D_x$
a (Å)	5.077(1)	5.404(1)	5.065(1)	5.376(1)	5.040(1)	5.347(1)	5.032(1)	5.330(1)	5.020(1)	5.316(1)
c (Å)	8.289(2)	8.821(2)	8.275(2)	8.788(2)	8.241(2)	8.745(2)	8.236(2)	8.719(2)	8.225(1)	8.694(2)
4f (1/3, 2/3, *z*)										
Zr *z*	0.0639(4)		0.0639(6)		0.0626(6)		0.0630(5)		0.0628(4)	
n	0.5		0.5		0.5		0.5		0.5	
2a (0, 0, 0)										
n Co	0.099(2)		0.125		0.125		0.125		0.125	
n V	0.151(3)		0.108(7)		0.063(6)		0.037(6)		0.011(4)	
n Cr	0.		0.017(7)		0.062(6)		0.088(6)		0.114(4)	
6h (*x*, 2*x*, 1/4)										
x	0.828(4)		0.825(4)		0.829(4)		0.829(2)		0.829(4)	
n Co	0.401(3)		0.375		0.375		0.375		0.375	
n V	0.349(3)		0.258(8)		0.176(8)		0.097(9)		0.033(7)	
n Cr	0.		0.117(8)		0.199(8)		0.278(9)		0.342(7)	
D1 (*x*, *y*, *z*)										
n =		0.79(4)		0.80(4)		0.81(2)		0.76(2)		0.66(2)
x =		0.042(2)		0.041(2)		0.046(2)		0.044(2)		0.046(2)
y =		0.325(2)		0.322(2)		0.327(2)		0.320(2)		0.321(2)
z =		0.561(2)		0.559(2)		0.565(2)		0.562(2)		0.564(2)
D2 (*x*, 2*x*, *z*)										
n =		0.43(2)		0.46(2)		0.48(2)		0.48(2)		0.43(2)
x =		0.448(4)		0.452(4)		0.453(4)		0.454(4)		0.457(4)
z =		0.630(2)		0.634(2)		0.634(2)		0.635(2)		0.634(2)
D3 (*x*, 2*x*, 1/4)										
n =		0.25(1)		0.25(1)		0.27(1)		0.27(1)		0.28(1)
x =		0.458(5)		0.459(5)		0.461(5)		0.461(5)		0.465(5)
D4 (*x*, 2*x*, 1/4)										
n =		0.18(1)		0.17(1)		0.15(1)		0.13(1)		0.08(1)
x =		0.199(8)		0.205(8)		0.210(9)		0.209(8)		0.209(9)
R_p (%)	1.6	1.8	2.1	2.1	1.7	1.8	2.4	1.8	1.5	1.8
R_{wp} (%)	2.1	2.4	3.1	3.2	2.2	2.4	3.0	2.5	1.9	2.4
R_B (%)	13.9	19.6	10.5	19.3	11.3	18.3	10.5	17.2	9.3	16.4
2a site	$Co_{0.20}V_{0.30}$		$Co_{0.25}V_{0.22}Cr_{0.07}$		$Co_{0.25}V_{0.12}Cr_{0.12}$		$Co_{0.25}V_{0.07}Cr_{0.18}$		$Co_{0.25}V_{0.02}Cr_{0.23}$	
6h site	$Co_{0.80}V_{0.70}$		$Co_{0.75}V_{0.52}Cr_{0.23}$		$Co_{0.75}V_{0.36}Cr_{0.40}$		$Co_{0.75}V_{0.19}Cr_{0.56}$		$Co_{0.75}V_{0.07}Cr_{0.68}$	
Refined formula	$ZrCo_{1.0}V_{1.0}$		$ZrCoV_{0.74}Cr_{0.30}$		$ZrCoV_{0.48}Cr_{0.52}$		$ZrCoV_{0.26}Cr_{0.74}$		$ZrCoV_{0.09}Cr_{0.91}$	
x (D) =		3.30(16)		3.36(16)		3.42(16)		3.29(12)		2.90(10)

model as for the corresponding alloys. Hydrogen accommodates in the A2B2 sites, the most attractive sites in the structure. The hydrogen atoms are located on four tetrahedral sites using the notations of Shoemaker [1]: D1 (24l), D2 ($12k_2$), D3 ($6h_1$) and D4 ($6h_2$) all with a [2Zr–2M] environment, in agreement with the positions determined by Didisheim in $ZrMn_2$ [3]. The D1 site is found the most occupied together with the D2 and D3 sites, the D4 site being the less occupied and the first to be emptied when the total hydrogen capacity is reduced ($x = 0.8$). All along the refinement procedure, the total hydrogen content has been free to vary, we have obtained hydrogen total occupations very close to the ones measured by the weighing procedure. The final refined parameters for the hexagonal hydrides are reported in Table 2. Fig. 2b reports the experimental refined pattern of the $ZrCoV_{0.2}Cr_{0.8}D_3$ deuteride.

3.3. *P–c–T diagrams*

In Fig. 4 we have plotted absorption–desorption isotherms measured at temperatures ranging from 50 to 150°C for $ZrCoV_{0.2}Cr_{0.8}$. These curves were recorded after ten cycles of absorption–desorption between 25 and 200°C. The hydride shows a rather flat plateau pressure at 50°C close to 0.1 MPa with a totally reversible hydrogen release. At 100°C, the plateau pressure is close to 0.25 MPa and the reversible hydrogen capacity is 2.6 H/f.u. The activation energy measured from an Arhenius plot is −0.624 Kcal/mole.

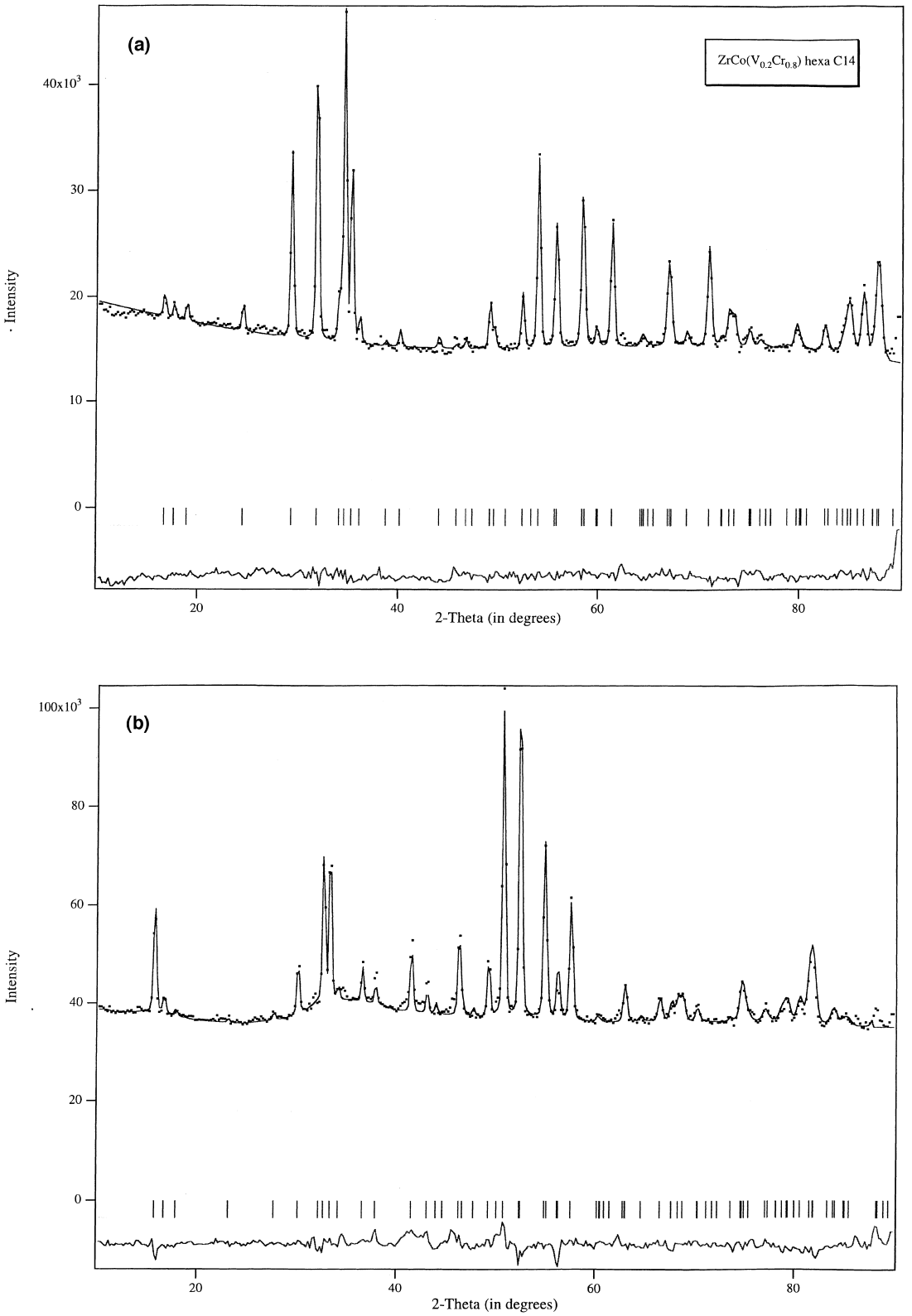

Fig. 2. Powder neutron diffraction pattern recorded at $\lambda = 1.288$ Å and room temperature. ·: experimental points; -: calculated intensities; |: line positions. The difference between the observed and calculated values is shown at the bottom: (a) $ZrCoV_{0.2}Cr_{0.8}$ as cast alloy; (b) $ZrCoV_{0.2}Cr_{0.8}D_3$ deuteride.

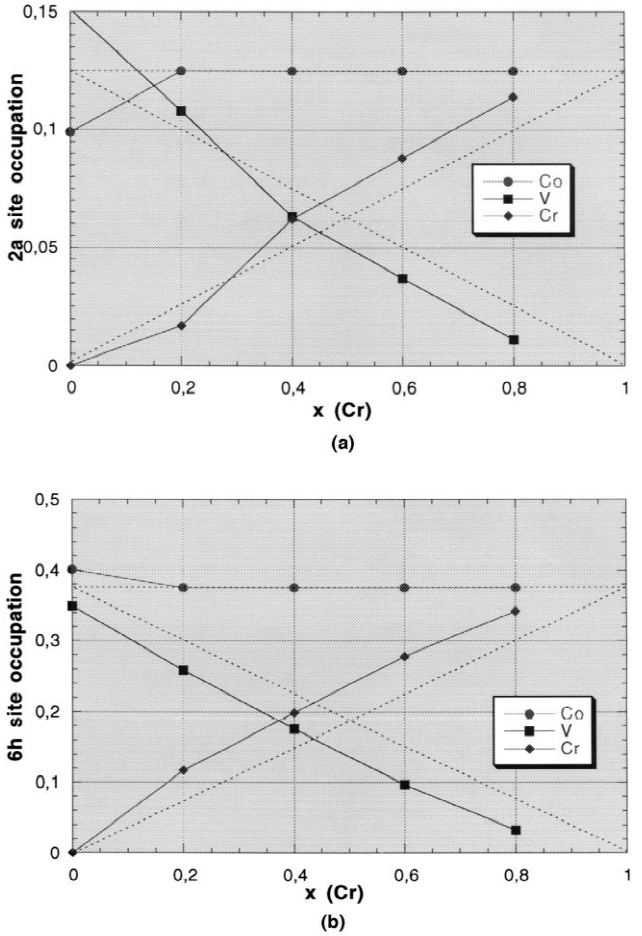

Fig. 3. Composition dependence of the occupation of crystallographic sites by transition metal atoms in $ZrCoV_{1-x}Cr_x$ compounds at room temperature as determined by neutron diffraction.

4. Conclusion

We have synthesised Laves phase compounds $ZrCoV_{1-x}Cr_x$ in the composition range $0 \leq x \leq 1$. The as-cast alloys crystallise in the C14 hexagonal structure with a decrease in the unit cell volume versus the chromium content. The number of absorbed hydrogen atoms in the $ZrCoV_{1-x}Cr_x$ alloys reaches large values but varies moderately versus the chromium substitution ($H/M > 1.1$). Hydrogen occupies the most attractive A2B2 sites with a preference hierarchy $D1 > D2 > D3 > D4$. The total occupancy measured by neutron diffraction is found in good agreement with the weighing procedure. The decrease in the hydrogen content is mainly due to the decrease of the volume cell of the alloy with the V by Cr substitution and subsequently to the hole size of the different interstitials sites [22].

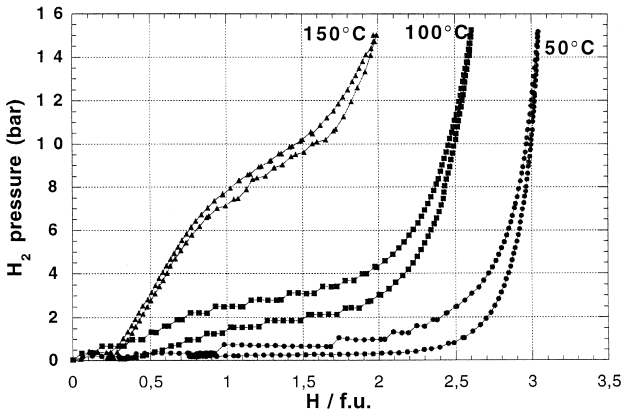

Fig. 4. *P–c–T* curves recorded between 0 and 15 bar at different temperatures for the compound $ZrCoV_{0.2}Cr_{0.8}$.

References

[1] D.P. Shoemaker, C.B. Shoemaker, J. Less-Comm. Met. 68 (1979) 43.
[2] D. Fruchart, A. Rouault, C.B. Shoemaker, D.P. Shoemaker, J. Less-Comm. Met. 73 (1980) 363.
[3] J.J. Didisheim, K. Yvon, D. Shaltiel, P. Fischer, Solid State Comm. 31 (1979) 47.
[4] A. Pebler, E.A. Gulbransen, Electrochemical Technology 4 (5-6) (1966) 211.
[5] D. Shaltiel, I. Jacob, D. Davidov, J. Less-Comm. Met. 53 (1977) 117.
[6] A. Perevesenzew, E. Lanzel, O.J. Eder, E. Tuscher, P. Weinzierl, J. Less-Comm. Met. 143 (1988) 39.
[7] I. Jacob, D. Shaltiel, D. Davidov, I. Miloslavski, Solid State Comm. 23 (1977) 669.
[8] D.G. Ivey, D.O. Northwood, J. Less-Comm. Met. 115 (1986) 295.
[9] S. Qian, D.O. Northwood, J. Less-Comm. Met. 147 (1989) 149.
[10] M. Boulghallat, N. Gerard, O. Canet, A. Percheron-Guegan, Z. Phys. Chem. NF 179 (1993) 171.
[11] S. Hirosawa, F. Pourarian, V.K. Sinha, W.E. Wallace, J. Magn. Magn. Mat. 38 (1983) 159.
[12] A. Drasner, Z. Blazina, J. Less-Comm. Met. 163 (1990) 151.
[13] S.R. Kim, J.Y. Lee, J. Alloys Comp. 185 (1992) L1.
[14] A. Drasner, Z. Blazina, J. Less-Comm. Met. 175 (1991) 103.
[15] I. Jacob, D. Shaltiel, in: T.N. Veziroglu, W. Seifritz (Eds.), Hydrogen Energy Systems, Pergamon, Oxford, 1979, p. 1689.
[16] J.L. Soubeyroux, M. Bououdina, D. Fruchart, L. Pontonnier, J. Alloys Comp. 219 (1995) 48.
[17] J.L. Soubeyroux, M. Bououdina, D. Fruchart, P. de Rango, J. Alloys Comp. 231 (1995) 760.
[18] M. Bououdina, J.L. Soubeyroux, D. Fruchart, E. Akiba, K. Nomura, J. Alloys Comp. 235 (1996) 93.
[19] M. Bououdina, J.L. Soubeyroux, D. Fruchart, Int. J. Hydrogen Energy 22 (1997) 329.
[20] M. Bououdina, P. de Rango, D. Fruchart, J.L. Soubeyroux, J. Alloys Comp. 253–254 (1997) 221.
[21] M. Bououdina, P. Menier, J.L. Soubeyroux, D. Fruchart, J. Alloys Comp. 253–254 (1997) 302.
[22] M. Bououdina, J.L. Soubeyroux, D. Fruchart, P. de Rango, J. Alloys Comp. 257 (1997) 82.
[23] J. Rodriguez-Carvajal, Proceedings of the Fifteenth Congress Int. Union of Crystallography, Satellite Meeting on Powder Diffraction, Toulouse, 1990, p. 127.
[24] M. Bououdina, J.L. Soubeyroux, P. Juen, C. Mouget, R. Argoud, D. Fruchart, J. Alloys Comp. 231 (1995) 422.